Membrane and Water Treatment, *Vol. 16, No. 1 (2025) 29-40*
https://doi.org/10.12989/mwt.2025.16.1.029

Mixed matrix PES membranes incorporated with rGO and f-rGO with improved metal removal capacity

Dixita P. Prajapati[a] and C.N. Murthy[*]

Macromolecular Materials Laboratory, Applied Chemistry Department, Faculty of Technology and Engineering, The Maharaja Sayajirao University of Baroda, Vadodara, Gujarat, India, 390001

(Received April 17, 2024, Revised October 9, 2024, Accepted October 10, 2024)

Abstract. In this work graphene oxide (GO) was synthesized and reduced to obtain reduced graphene oxide (rGO), which was further functionalized to obtain functionalized reduced graphene oxide (f-rGO). The performance of membranes was studied in terms of pure water flux and rejection of heavy metal. The resulting membranes showed improved water permeability, heavy metal rejection, and antifouling properties compared to pristine polyethersulfone membranes. These enhancements were attributed to increased hydrophilicity and smoother surfaces facilitated by the graphene derivatives which was analysed by contact angle analyser, atomic force microscopy and field emission scanning electron microscopy. Functionalized reduced graphene oxide containing polyethersulfone membrane gives increased water flux reaching a maximum of 257 LMH ($L/m^2.h$) and higher metal removal nearly 86% rejection for Pb (II), 92% rejection for Cu (II) and 95% rejection for Cr (VI) as well as increased bovine serum albumin rejection of 94.2% along with 80.5% flux recovery ratio which is higher than reduced graphene oxide containing polyethersulfone and pristine polyethersulfone membranes. Overall, functionalized reduced graphene oxide containing polyethersulfone membranes exhibited the best performance, making them promising for various separation applications.
Keywords: antifouling; functionalized reduced graphene oxide; graphene oxide; mixed matrix membranes; reduced graphene oxide

1. Introduction

These days, freshwater scarcity is becoming a global issue. The rapid advancement of the economy, population expansion, and industrial growth contribute to an increased demand for fresh water. Heavy metal contamination in wastewater is a significant worldwide issue due to its negative effects on water quality and exacerbation of water scarcity (Li and Tian 2021, Nompumelelo *et al.* 2023). Water distribution systems often contain a variety of heavy metal ions, including lead, chromium, copper, arsenic, cadmium, zinc, nickel, mercury, and cobalt. Heavy metals are resistant to biodegradation and possess potential carcinogenic properties (Moradi *et al.* 2020). The existence of these ions in wastewater has a negative impact on the ecosystem and also directly or indirectly affect the human health (Mukherjee *et al.* 2016, Nompumelelo *et al.* 2023, Qasem *et al.* 2021). Exposure to heavy metals can lead to serious health problems, such as cardiovascular issues, kidney problems, neurological disorders and cancer (Mondal and Majumder 2020). So, it is essential to remove heavy metals from wastewater to safeguard both the ecosystem and human health. The elimination of heavy metals from wastewater can be accomplished through conventional methods like chemical precipitation, ion exchange, electro-chemical removal, chemical adsorption, physical adsorption, ion exchange, flocculation, and biological growth (Nompumelelo *et al.* 2023). But the practical application of these techniques is limited due to several drawbacks, such as the generation of toxic sludge, incomplete removal, substantial energy demands, pre and post-processing requirements, and high operating costs (Mukherjee *et al.* 2016, Sogut *et al.* 2020, Bhol *et al.* 2021). As a result, an effective, high throughput and low energy consuming heavy metal removal techniques are required. A more eco-friendly and efficient solution to tackle this problem entails employing membrane separation techniques for the reclamation of wastewater.

Membrane separation technique has gained popularity for the treatment of wastewater due to its ability to remove suspended solids, organic compounds, and heavy metals and also due to its ease of operation, low operating costs and high energy efficiency (Baraka 2011, Li and Tian 2021). Reverse osmosis, ultrafiltration, and nanofiltration are three different techniques for metal separation where membrane technology has become more commonly used (Bakshi *et al.* 2021, Giwa *et al.* 2019). The most commonly used polymers in the production of commercial and laboratory nanofiltration membranes are polyethersulfone (PES), polysulfone (PS), polyvinylidene fluoride (PVDF), cellulose acetate (CA), polyurethane (PU) etc. (Giwa *et al.* 2019, Aziz *et al.* 2019).

PES stands out for membrane applications due to its high mechanical strength, thermal stability, excellent chemical resistance, biocompatibility, tunable surface

[*]Corresponding author, Professor,
E-mail: chivukula_mn@yahoo.com
[a] Ph.D. Student, E-mail: prajapatidixita2509@gmail.com

ISSN: 2005-8624 (Print), 2092-7037 (Online)

properties and easy processing. However, PES membrane suffers from fouling because of its hydrophobic properties, which will impact the performance of the membrane. Fouling is a serious issue in PES membranes, which negatively impacts membrane performance leading to decrease in water permeability (Forati *et al.* 2014, Razmjou *et al.* 2012, Van der Bruggen 2009). A number of techniques have been proposed to reduce membrane fouling, including blending with hydrophilic polymers (Peyravi *et al.* 2012, Rahimpour and Madaeni 2007), grafting with hydrophilic monomers (Rahimpour 2011, Seman *et al.* 2012), grafting with short-chain molecules (Shi *et al.* 2011), embedding hydrophilic nanoparticles (Vatanpour *et al.* 2012a), etc. Among the many strategies to control membrane hydrophilicity and fouling, mixing inorganic nanomaterials has garnered a lot of interest. Various types of nanomaterials like TiO_2 nanoparticles (Wu *et al.* 2008), Fe_3O_4 nanoparticles (Alam *et al.* 2013), CuO nanoparticles (Nasrollahi *et al.* 2019), ZnO nanoparticles (Shen *et al.* 2012), silver nanoparticle (Sonawane *et al.* 2017), manganese oxide nanoparticles (Gohari *et al.* 2014) etc are incorporated into the polymer matrices for the modification of membranes. This is attributed to an enhancement in hydrophilicity and alteration in membrane morphology (Zinadini *et al.* 2014).

Recently 2-D graphene-based nanomaterial has attracted a significant attention to use as a filler in membrane preparation due to its high surface area, mechanical strength, chemical inertness, excellent thermal stability, tunable properties, and antibacterial qualities (Jamil *et al.* 2019). Graphene oxide (GO) is a promising material for creating graphene-based separating membranes with high water flux. The main drawback of using GO in membrane preparation is its tendency to swell in water due to the presence of oxygen containing functional groups like carboxyl, hydroxyl and epoxide, which results in enlargement of the nanochannels leading to decrease in stability and selectivity of the membranes (Lin *et al.* 2018). A number of techniques have been used to increase the stability of GO membranes, including cross-linking methods by ions, amide and esterification reactions (Jia and Wang 2015) and reduction of GO to reduced graphene oxide (rGO). GO laminates undergo chemical reduction to eliminate hydrophilic functional groups. This process enhances the stability of GO laminates and reduces the size of nanochannels, leading to improved rejection of ionic species during desalination. However, the narrowed nano-channels and hydrophobic surface of rGO laminates may pose obstacles to water transport. Therefore, the control on degree of reduction is necessary to produce the rGO membranes with good water permeability and enhanced metal removal capacity (Bakshi *et al.* 2021, Li *et al.* 2019).

Furthermore, studies have indicated that the rapid water flow within the core of carbon nanotubes (CNTs) is attributed to the hydrophobic inner surface of the CNTs. However, the highly hydrophobic entrance of CNTs impedes easy entry of water into their core. Previous research has addressed this issue by introducing hydrophilic functional groups to mitigate entrance resistance (Hou *et al.* 2010, Shah and Murthy 2013). if the surface of the laminates is more hydrophilic, water may flow easily through the nanochannels formed in rGO laminates. Therefore, functionalization of rGO was carried out. Prior research findings (Table 1.) have indicated that incorporation of rGO in polymer matrices leads to decrease in pure water flux so to overcome this problem controlled reduction of GO was carried out (Zhang *et al.* 2018). However, no reports are available to use functionalized rGO (f-rGO) in the preparation of mixed matrix membrane.

In present work, amine functionalization of rGO was carried out by using ethylenediamine to introduce hydrophilic amine functional group on the surface of the rGO laminate. On functionalization of rGO with ethylenediamine free - NH_2 group is obtained which increases the hydrophilicity of the material and making it more dispersible. So, the addition of amine functional group on rGO not only addresses the dispersion and compatibility issues associated with traditional fillers but also improves the hydrophilicity, selectivity, stability and mechanical strength of the membrane, making it a promising material for advanced separation processes. The functionalization of rGO with amine groups is a strategic approach to enhance the performance of PES mixed matrix membranes. The potential of utilizing rGO and f-rGO as inorganic nanofillers during the fabrication of PES mixed matrix membrane was investigated. The properties of as prepared GO, rGO and f-rGO were characterized using several techniques, i.e., fourier transform infrared spectroscopy (FTIR), raman spectroscopy, scanning electron microscopy (SEM) and energy dispersive X-ray spectroscopy (EDS). Then, rGO and f-rGO incorporated flat sheet polyethersulfone mixed matrix membranes (MMMs) were fabricated via phase inversion method. The synergistic effects of the nanofillers towards the structural properties of the fabricated membranes were then investigated by field emission scanning electron microscopy (FESEM) and atomic force microscopy (AFM). The findings of this study are expected to provide new insights for the development of advanced mixed matrix membranes capable of efficient metal removal and high pure water flux.

2. Experimental

2.1 Materials

Polyethersulfone (PES) was purchased from M/s Permionics Membranes Pvt., Ltd., Vadodara, India. potassium permanganate (Rankem), graphite fine powder (98%, Merck), concentrated sulphuric acid (98%, Merck), ortho phosphoric acid (Merck), hydrogen peroxide (30%, Rankem), 98% pure hydrochloric acid (37%, Merck), thionyl chloride (>99%, Sigma-Aldrich), ethylene diamine (99%, Merck), Dimethyl formamide (DMF) (98%, Merck) were used as received.

2.2 Preparation of Graphene Oxide (GO)

Different methods are used for the synthesis of graphene oxide such as Tour method, Brodie's method, Staudenmaier's method, Hummer's method, Improved Hummer's method (Adetayo and Runsewe 2019). Natural graphite powder is

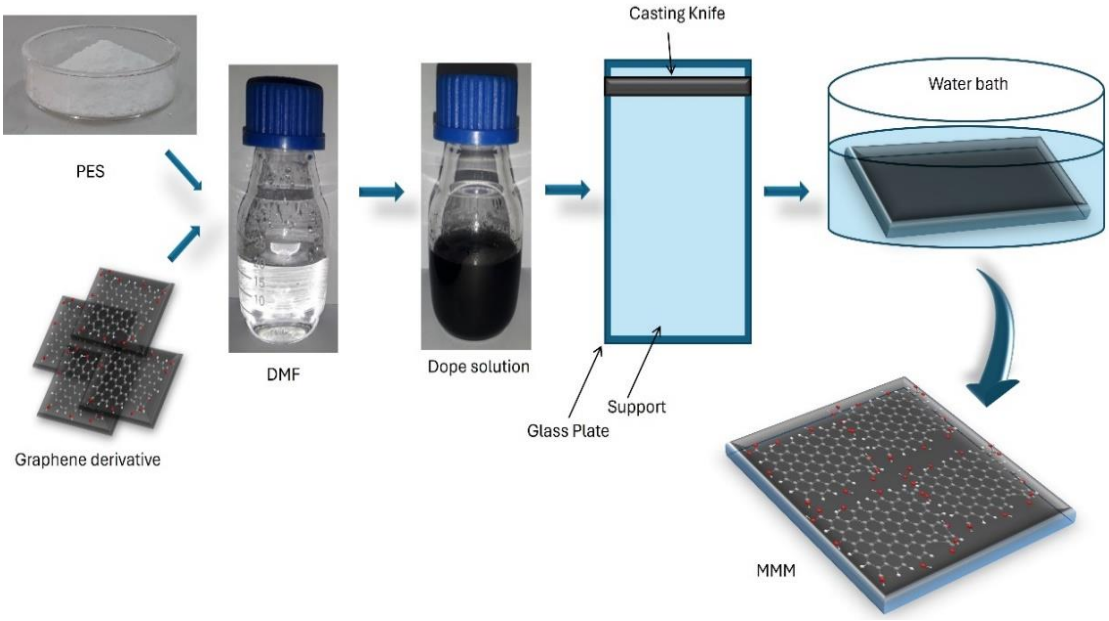

Fig. 1 Schematic representation of phase inversion technique

used as a raw material for the preparation of GO in all the above methods (Marcano *et al.* 2010).

In Improved Hummer's method a mixture of concentrated H_2SO_4/H_3PO_4 (9:1, 360:40 ml) was added into 3×10^3 mg graphite powder. Then 1.8×10^4 mg $KMnO_4$ was added slowly under constant stirring in an ice bath to maintain the temperature of the reaction below 30 ˚C. The reaction was then heated at 50 ˚C and stirred for 12 h. The reaction mixture was cooled at RT and then poured into the ice containing 3 ml 30% H_2O_2.The reaction mixture was allowed to settled overnight and supernatant decanted away. The remaining solid material was washed in series with 200 ml of water, 200 ml of 30% HCl and 200 ml of ethanol until neutral supernatant was obtained. The obtained solid was dried overnight at 45 ˚C in vacuum oven for 24 h.

2.3 Preparation of reduced Graphene Oxide (rGO)

In the preparation of rGO, first 1000 mg GO was dispersed in 500 ml of DI water by sonication for 2 h. Hydrazine hydrate was added drop wise into the dispersion of GO at room temperature and then reflux at 100 ˚C for 1 h. In this reaction the weight ratio of hydrazine hydrate and GO was maintained at 9:7 (Sharma *et al.* 2017). The brown colour of the GO was converted to black due to the removal of oxygen containing functional groups and reformation of л conjugated network during the reduction (Mungse and Khatri, 2014). The resultant reaction mixture was filtered through cellulose filter paper and washed with 1M HCl and DI water until neutral filtrate was obtained. The obtained product was dried at 40 ˚C in an oven for 24 h.

2.4 Preparation of functionalized Reduced Graphene Oxide (f-rGO)

For the preparation of f-rGO, rGO was treated with thionyl chloride for the conversion of carboxylic group into acyl chloride group. For that 500 mg rGO was dispersed in 20 ml DMF by sonication. Then 1.5 ml $SOCl_2$ was added drop wise and reflux at 60˚C for 36 h. The obtained product was filter and wash with toluene to remove the traces of $SOCl_2$. The product was dried in a vacuum oven at 80 ˚C for 4 h. 200 mg acylated rGO was dispersed in 25 ml of ethylene diamine by sonication and sonication was continued for 16 h at 35 ˚C. The product was filtered, washed with methanol and dried in a vacuum oven at 80 ˚C for 4 h.

2.5 Preparation of Mixed Matrix Membranes

Mixed matrix membranes were synthesized by using phase inversion technique (Fig. 1). First PES was dried in a vacuum oven at 80˚C for 24 h before use. In phase inversion process first appropriate amount of filler was dispersed in DMF by sonication and then known amount of polymer was dissolve in it (Table 2.) by stirring at 900 rpm. To get rid of the gas bubbles, the dope solution was rested for overnight before casting. A flat sheet membrane was casted on nomex sheet using glass plate as a support. For casting the membrane film applicator with the thickness of 200micrometer was used. The casted membrane was immediately immersed into a coagulation bath containing DI water where solvent-non-solvent exchange was carried out and the membrane of uniform thickness was prepared figure 1. The membrane was soaked in DI water for 24 h to ensure complete phase inversion. Then the membranes were removed from the DI water and dried in an oven at 40˚C.All the membranes were stored in DI water until it was used.

2.6 Permeation Test

The newly developed membranes' performance was evaluated by measuring pure water flux, salt rejection study and fouling behaviour. All permeation experiments were

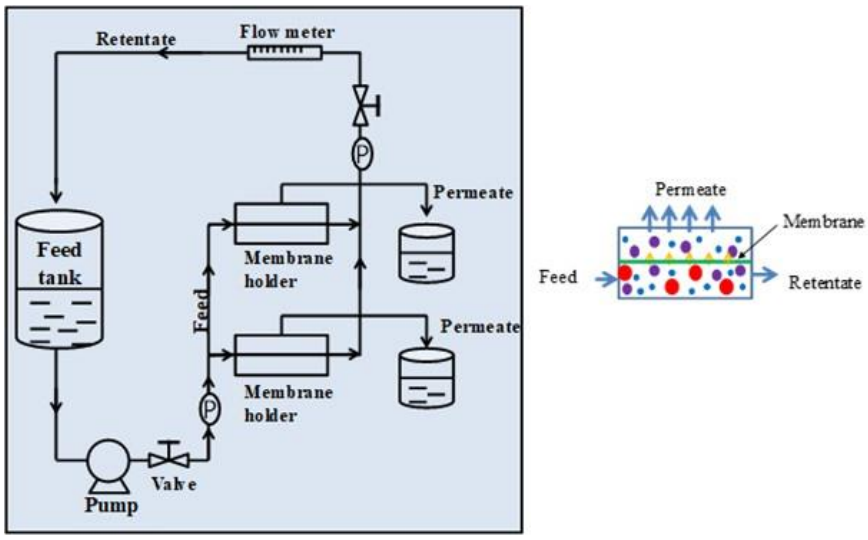

Fig. 1 Schematic representation of phase inversion technique

carried out on a crossflow filtration cell (Fig. 2) using circular membrane having 78.5 cm^2 effective area available for filtration. Commercial booster pump was used to circulate the feed solution in the filtration cell and transmembrane pressure was regulated by using outlet valve. The membranes were compacted for 1 hour at 50 psi pressure before starting the experiment. After stabilization permeate was collected to calculate the pure water flux and percentage removal of metal ions and bovine serum albumin (BSA).

The pure water flux and solute rejection was calculated by using the following Eqs. (1)-(2).

$$\text{Pure Water Flux } (J) = \frac{W}{A\Delta t} \quad (1)$$

where W is the volume of the permeate (L), A is the membrane effective area (m^2) and Δt is permeation time (h).

$$\text{Rejection } (\%) = \frac{C_f - C_p}{C_f} \times 100 \quad (2)$$

where C_f and C_p are the concentration of feed and permeate solution respectively, measured by PerkinElmer Atomic Absorption Spectrometer PinAAcle™ 500. "PerkinElmer" from PerkinElmer, Inc., 940 Winter Street Waltham, MA 02451 USA. 298809 (012087B_01) PKI installed at Department of Environmental Studies, Faculty of Science, The Maharaja Sayajirao University of Baroda, Vadodara, Gujarat, India. UV Spectrometer was used to determine the feed and permeate concentration of bovine serum albumin (Nikita *et al.* 2020). After completion of BSA rejection experiment the membranes were backwashed with DI water for 1 h and pure water flux of cleaned membranes (J_2) was measured. To study the fouling behaviour of membranes in more detail the flux recovery ratio (FRR) and the irreversible fouling ratio (Rir) were calculated by using the following Eqs. (3)-(4).

$$\text{Flux recovery ratio (FRR)}(\%) = \frac{J_2}{J_1} \times 100 \quad (3)$$

$$\text{Irreversible fouling ratio (Rir)}(\%) = \frac{J_1 - J_2}{J_1} \times 100 \quad (4)$$

were J1 and J2 are pure water flux of the membranes before and after protein filtration respectively.

2.7 Characterization

GO, rGO, f-rGO and all the membranes were inspected by using various analytical techniques. Different functional groups present in GO, rGO and f-rGO were studied by using FTIR spectroscopy (Bruker spectrometer as KBr pellets). Raman Spectroscopy (Raman Spectrometer Airix Corporation/ Technos Instruments formerly Seki Technotron Corp./ Cornes Technologies Ltd. STR 300 Raman System) was used to analyse the Structural changes carried out during the synthesis of GO, rGO and f-rGO. Morphology and chemical composition of prepared nanomaterial was studied by using SEM and EDS (SIGMA 500VP Field Emission Scanning Electron Microscope with EDS and EBSD Sensors at NIT Jalandhar). Morphology of all fabricated membranes was studied by using AFM (WITEC Alpha300 RA – Confocal Raman Microscope with AFM at SAIF Kottayam) and FESEM (JEOL JSM-7600F FEG-SEM at IIT Bombay, Maharashtra, India). Hydrophilicity of the membranes were checked by contact angle measurement (Dataphysics DSA10- MK2 (Krüss, Germany) using CA measurement system installed at Department of Chemistry NIT Jalandhar). Pure water flux, rejection of heavy metals and BSA was performed on stainless steel membrane test cell fabricated in house.

3. Result and discussion

3.1 FTIR spectroscopy

The FTIR spectra of GO shows a broad and intense band at 3430 cm^{-1} due to the stretching vibration of –OH group. Bands at 1732 cm^{-1} arises due to the C=O stretching

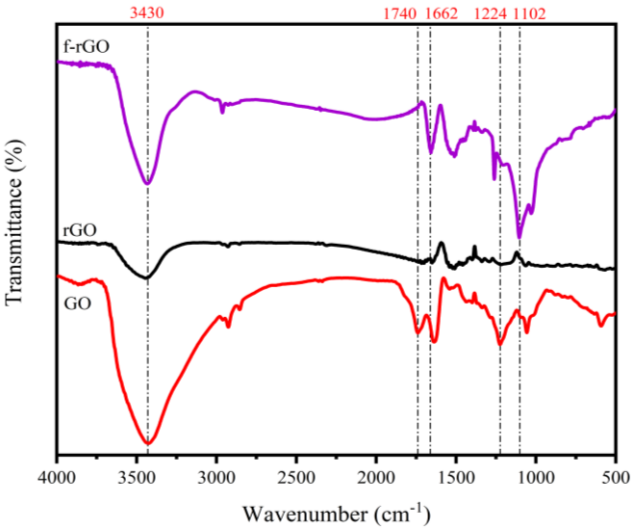

Fig. 3 FTIR Spectra of GO, rGO and f-rGO

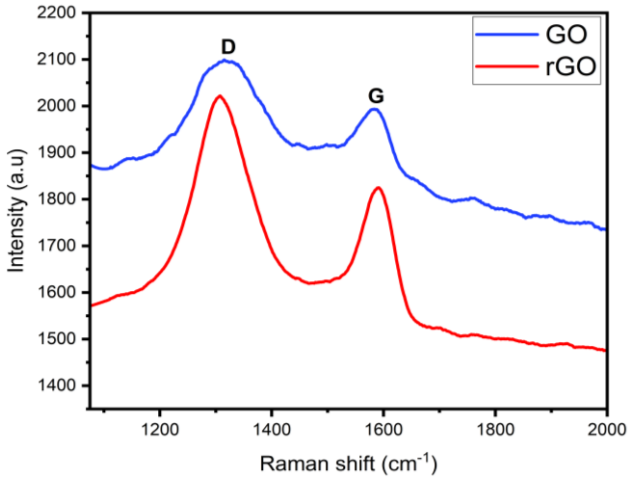

Fig. 4 Raman spectra of GO, rGO and f-rGO

of carboxylic group, 1636 cm^{-1} arises due to the C=C aromatic stretching of sp2 carbon, 1216 cm^{-1} and 1060 cm^{-1} arises due to the C – O stretching of hydroxyl group and epoxide group respectively. In rGO all the bands attributed to the oxygen containing functional groups were obtained at lower intensity as compare to GO (Al-Naddaf *et al.* 2018). In f-rGO a sharp band arises at 3439 cm^{-1} due to N–H stretching vibration of $–NH_2$ group. In the spectra of f-rGO the band at 1732 cm^{-1} disappear and a new band at 1661 cm^{-1} is appear due to the amide carbonyl stretching (Shah and Murthy 2013). The bands at 1504 cm^{-1} assigned to the overlap signature of N-H bond and C=C aromatic stretching of sp2 carbon of rGO skeleton (Mungse and Khatri, 2014), 1254 cm^{-1}, 1020 cm^{-1} arises due to the C – O stretching of hydroxyl group and epoxide group respectively and 1102 cm^{-1} arises due to N – H stretching of aliphatic primary amine (Fig. 3).

3.2 Raman spectroscopy

Raman spectroscopy was used to determine the structural and compositional features of the samples (Sharma *et al.* 2017). Raman spectra of GO and rGO were recorded at 532 nm and 785 nm laser wavelength. The structural changes produced into GO and rGO through oxidation and reduction reaction was observed using Raman spectroscopy. Fig. 4 shows the Raman spectra of GO and rGO at 785 nm wavelength of laser. In GO two characteristic bands were obtained at 1320 cm^{-1} (D band) and 1584 cm^{-1} (G band) and in rGO the bands were obtained at 1307 cm^{-1} (D band) and 1588 cm^{-1} (G band). The D band arises due to the disordered structure of graphene and the G band arises due to the stretching vibration of C=C bond in graphitic material (li). From the spectrum it was observed that both the D and G bands were broader in GO than rGO which is due to the large number of sp2 domain present in GO. The relative intensity ratio (I_D/I_G) was calculated to evaluate the density of defects in sp2 carbon atom. The value of I_D/I_G increases due to the increase in defects (Sharma *et al.* 2017).

3.3 Scanning electron microscopy and Energy dispersive X-ray spectroscopy

The morphology of GO, rGO and f-RGO nanomaterial were examined by using SEM. The SEM micrographs provide a greatly enlarged image of the material's surface. As depicted in the Fig. 5(a), GO exhibits a sleek surface with curled edges. This corresponds to the presence of oxygen-containing functional groups, such as carboxyl (-COOH), hydroxyl (-OH), and epoxy (C-O-C) groups. which induce changes in the sp2 carbon structure on the basal plane. Bright silky edges of GO are noticeable due to the presence of various defects within the structure of graphene oxide (Jafari *et al.* 2022, Sheshmani and Fashapoyeh, 2013).

The SEM image of rGO (Fig. 5(b)) displayed a wrinkle structure, attributed to the swift elimination of oxygen-containing functional groups present in GO (Sharma *et al.* 2017, Zhou *et al.* 2011). According to Fig. 5(c) f-rGO exhibit more wrinkled structure due to the random orientation of aggregated domains in f-rGO (Das and Yurtcan 2022 Irani *et al.* 2018). Which resulted in increased surface roughness after functionalization.

Elemental analysis of the synthesized GO, rGO and f-rGO was conducted using EDS. EDS allows for the estimation of the elemental composition of the samples. Fig. 5 (d)-(f) represent the EDS spectra of GO, rGO and f-rGO. EDS spectra of GO and rGO (Fig. 5(d)-(f)) show a decrease in oxygen content from 44.02% to 11.12% which was due to the reduction of graphene oxide (Bora *et al.* 2013, Das and Yurtcan 2022). As shown in EDS spectra of f-rGO (Fig. 5(c)), 10.37% nitrogen content was present which indicates the successful functionalization of rGO.

3.4 Atomic force microscopy

AFM was used to study the surface roughness of the prepared membranes. In three-dimensional AFM images, the dark areas depict the pores or valleys of the membrane, whereas the brighter areas represent the highest points of the membrane surface. The two-dimensional and three-dimensional AFM images of pristine PES, rGO/ PES and

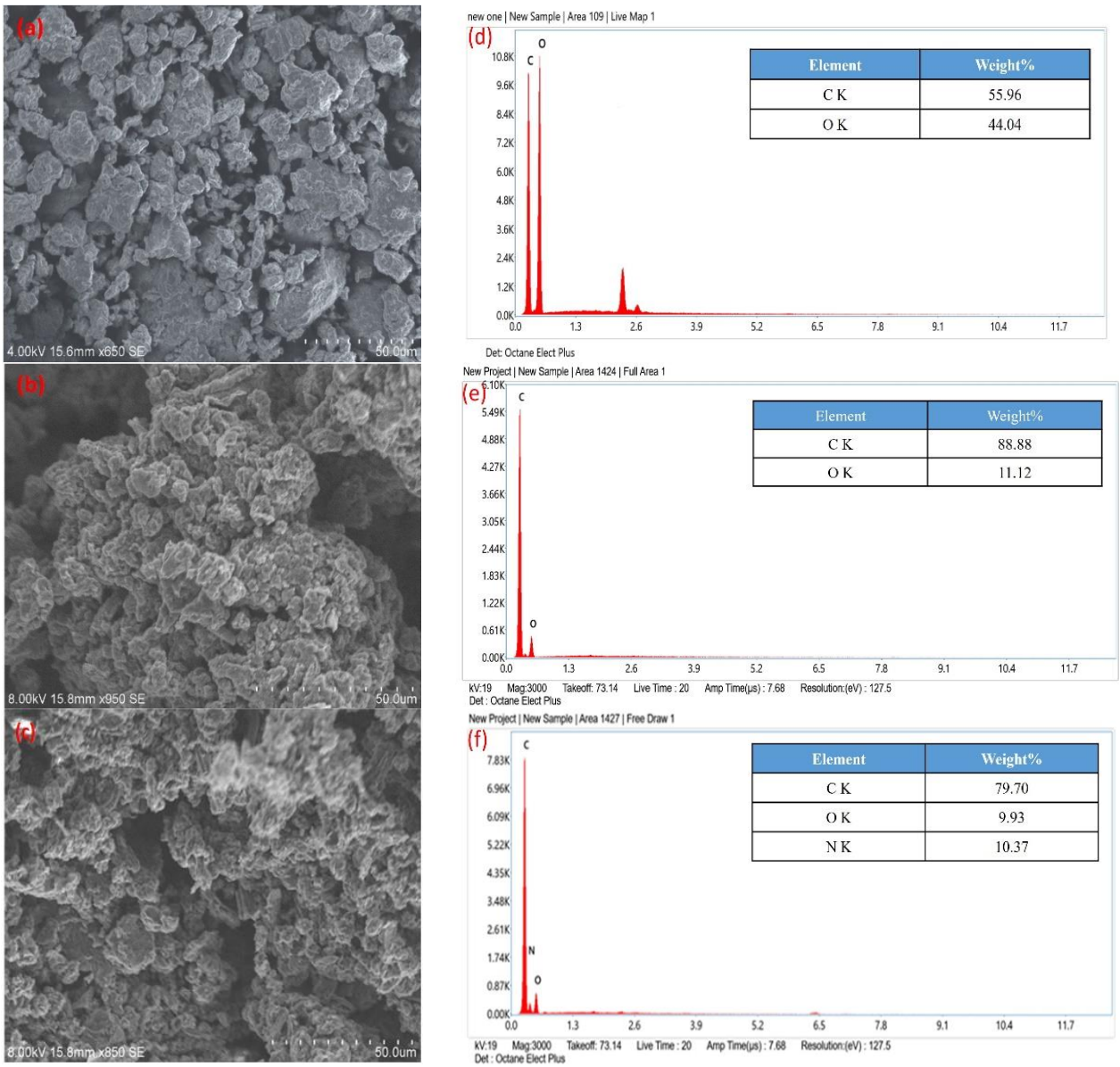

Fig. 5 SEM images of (a) GO, (b) rGO and (c) f-rGO and EDS spectra of (d) GO, (e) rGO and (d) f-rGO

Table 2 Properties of the membrane (GVHP, Millipore)

Membranes	Average roughness Sa (nm)	Root mean square Sq (nm)
PES	13.04 ± 0.22	20.10 ± 0.40
rGO/PES	6.27 ± 0.05	10.21 ± 0.089
f-rGO/PES	6.94 ± 0.04	13.80 ± 0.10

f-rGO/ PES membranes top surfaces are displayed in Fig. 6. The results demonstrated that the addition of rGO and f-rGO significantly altered the surface morphology. Introduction of functional groups during rGO functionalization can alter surface properties and decrease surface roughness. The surface roughness of the bare PES membranes was noticeably greater compared to those mixed with rGO and f-rGO. The incorporation of rGO and f-rGO resulted in the replacement of large peaks and valleys with numerous smaller ones, ultimately leading to a smoother membrane surface (Abdalla *et al.* 2020, Jafari *et al.* 2022, Safarpour *et al.* 2014, Vatanpour *et al.* 2020).

The surface roughness parameters of all the prepared membranes are outlined in Table 3, were calculated by using an AFM analysis software in an AFM scanning area of 6 µm x 6 µm. The bare PES membrane displays relatively high roughness measurements, with an average roughness (Sa) of 13.04 ± 0.22 nm and a root-mean-square roughness (Sq) of 20.10 ± 0.40 nm. These values suggest a surface characterized by notable height discrepancies and irregularities, likely stemming from inherent material properties such as surface imperfections and structural features. In contrast to the pristine PES membrane, the rGO/PES membrane exhibits a significant reduction in both average roughness (6.27 ± 0.05 nm) and root-mean-square (10.21 ± 0.089 nm).

This considerable decrease in roughness values signifies a substantial smoothing effect attributed to the inclusion of

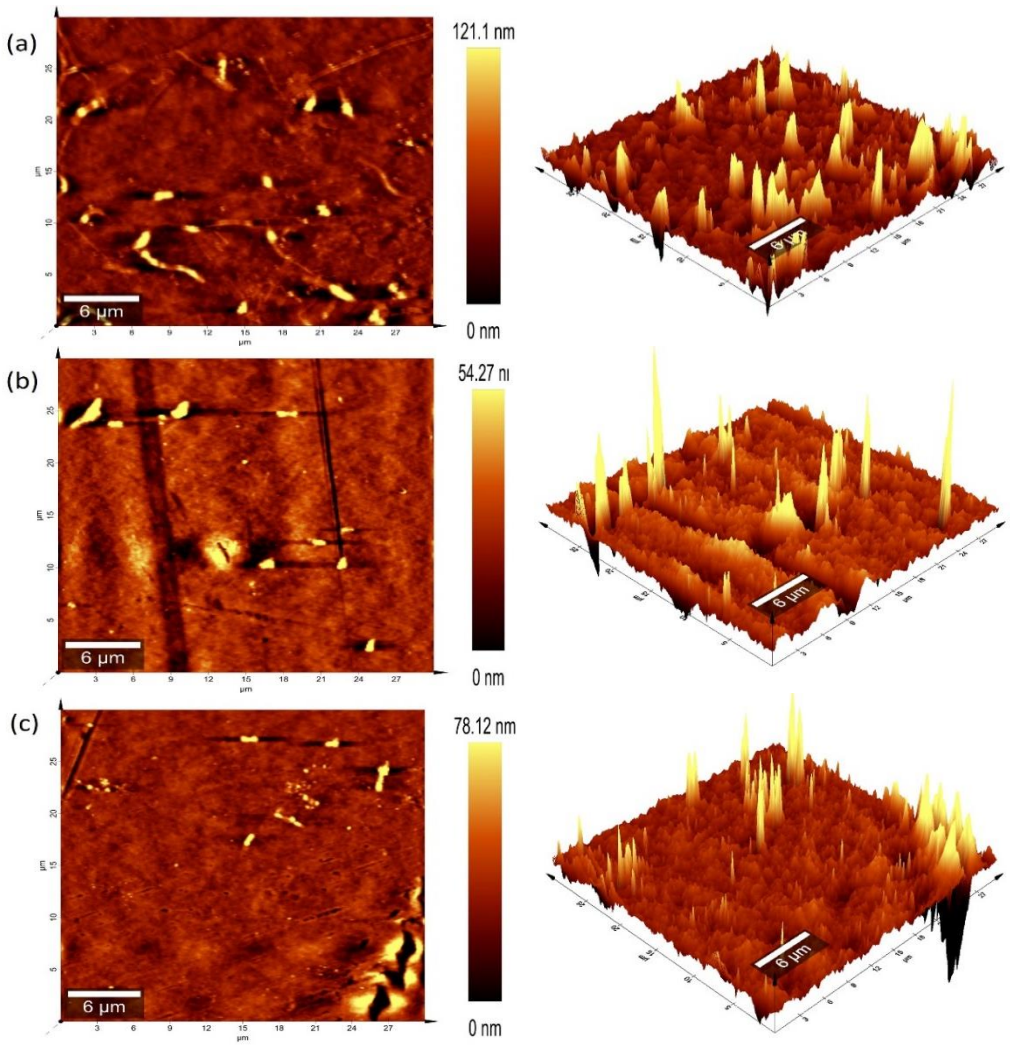

Fig. 6 Two-dimensional and three-dimensional AFM images of (a) PES, (b) rGO/PES and (c) f-rGO/PES membranes

rGO. The presence of carboxyl and hydroxyl functional groups on rGO appears to have filled surface defects and irregularities, resulting in a more homogeneous surface. Whereas in case of f-rGO/PES membrane the average surface roughness (6.94 ± 0.04 nm) and root mean square (13.80 ± 0.10 nm) are slightly increase compared to rGO/PES membrane. This could be due to the rapid solvent and non-solvent exchange during the phase inversion process, likely facilitated by the hydrophilic properties of f-rGO.

3.5 Field emission scanning electron microscopy

The morphology of the produced membranes was examined using surface topography and cross-sectional SEM images. Fig. 7 displays the SEM images showcasing the pores on the membrane surface and cross-sectional view of pristine PES, rGO/PES, and f-rGO/PES membranes. It could be clearly seen that the pristine PES membrane has larger pores and rough surface whereas rGO/PES and f-rGO/PES membranes have smaller pores and smooth surface as illustrated in Fig. 7 (a)-(f) clear finger like structure was observed in the cross-sectional SEM image of all the prepared MMMs. The cross-section analysis reveals that the finger-like pores do not exhibit any visible presence of rGO and f-rGO within the rGO/PES and f-rGO/PES membrane. However, this absence of observable rGO and f-rGO within the pores does not imply the absence of nanomaterials within the polymer matrix. This is due to the small size of the nanomaterials (Chai *et al.* 2017, Aziz *et al.* 2019). From the Fig. 7(f) we can see that the wider finger like pores were formed in f-rGO/PES membrane (Hamzah *et al.* 2020). This phenomenon can be elucidated by the abundance of various hydrophilic groups present in f-rGO, which facilitate an accelerated transfer between the solvent and non-solvent during phase inversion. As a result, the enlargement of pores and channels can be attributed to this swift mass exchange, which significantly influences the structure of the final f-rGO/PES membrane.

3.6 Hydrophilicity of the membranes

The hydrophilic properties of the prepared membranes were assessed using CA measurement system. The contact angle value of pristine PES membrane was 81.1° (Fig. 8(a)) which decreases to 68.0° (Fig. 8(b)) by the incorporation of

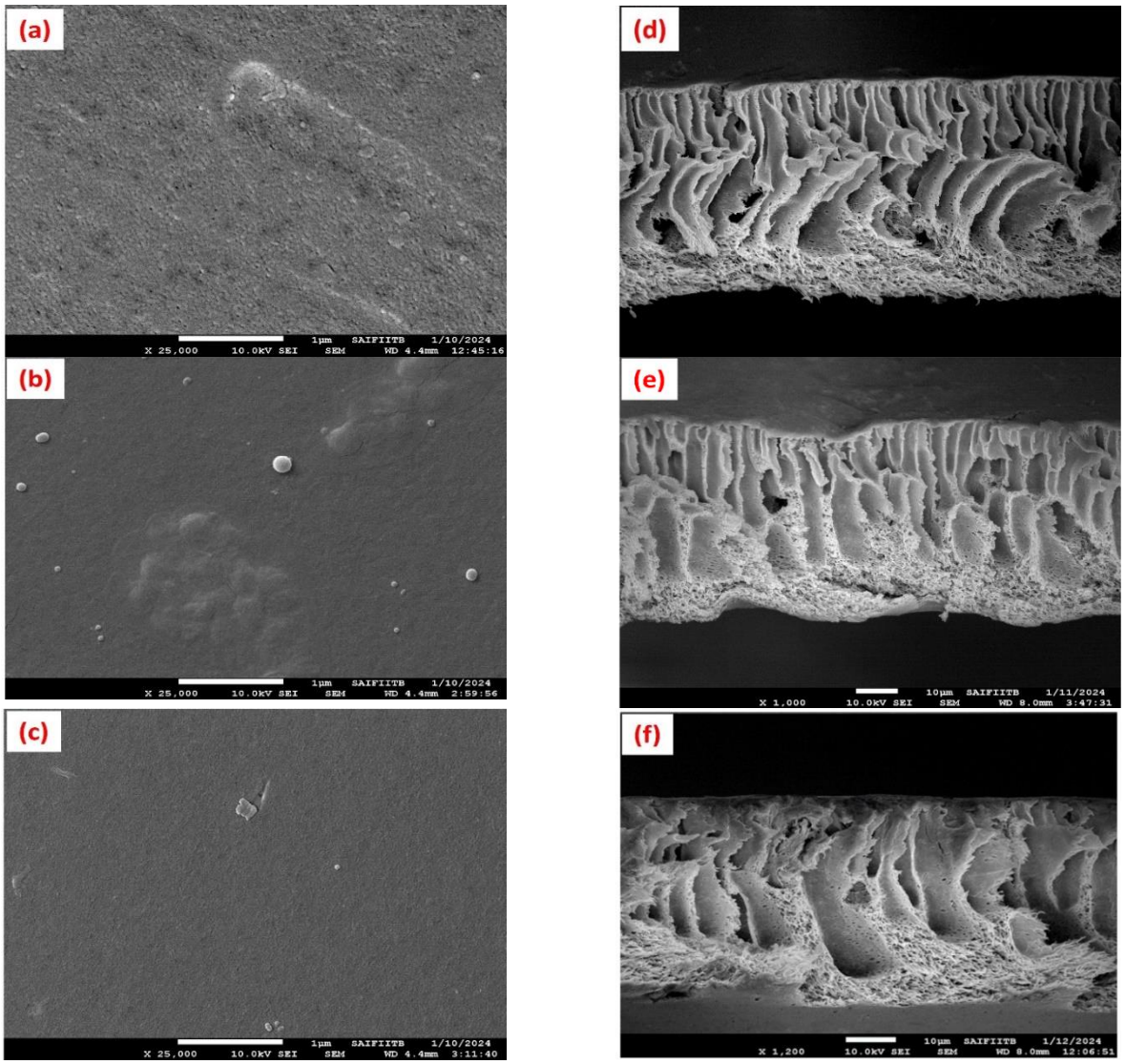

Fig. 7 Top surface and cross-section FESEM micrographs of (a, b) pristine PES, (c, d) rGO/PES, and (e, f) f-rGO/PES membranes

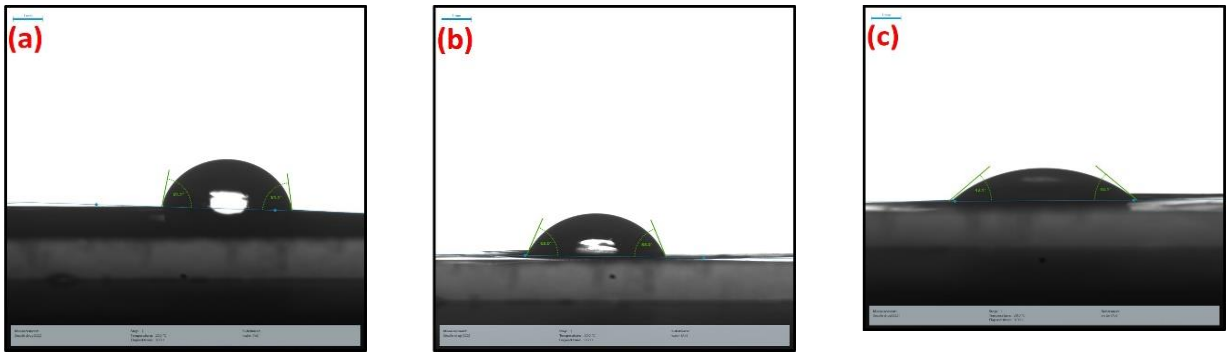

Fig. 8 Contact angle of (a) bare PES membrane, (b) rGO incorporated PES membrane and (c) f-rGO incorporated PES membrane

rGO into the polymer matrix. The hydrophilicity of rGO/PES membrane was increased due to the good interaction between PES and rGO. In the phase inversion process, rGO shifts towards the surface of the membrane to reduce interfacial energy (Zinadini *et al.* 2014). The hydrophilicity of the f-rGO/PES membrane was also increased which leads to decrease in the water contact angle value up to 43.1° (Fig. 8(C). Introduction of amine functional groups in rGO enhances surface polarity and interaction with polar solvents. f-rGO exhibits a strong attraction towards water

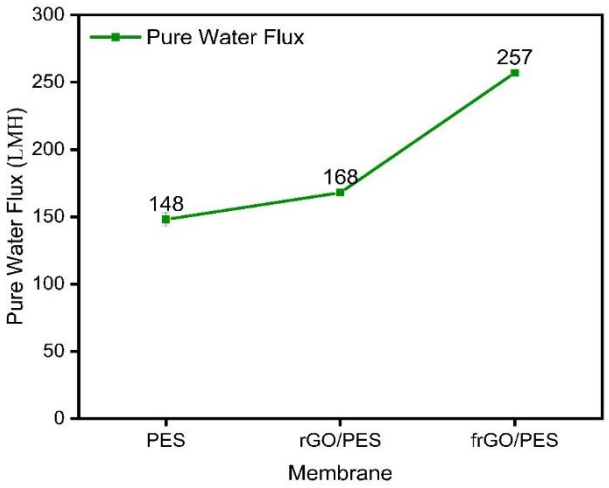

Fig. 9 Pure water flux of the membranes at 35 ℃ temperature

due to the presence of hydrophilic groups, so that the f-rGO swiftly moves towards the membrane/water interface during phase inversion process (Celik *et al.* 2011, Ganesh *et al.* 2013), thereby reducing the interfacial energy and resulting in increased hydrophilicity. The progression from pristine PES to f-rGO/PES membranes involves increasing surface hydrophilicity and reactivity, expanding the range of potential applications towards more selective and efficient separation processes.

3.7 Permeation study

To study the impact of rGO and f-rGO on the water permeability of PES membrane, membranes with 1.0% rGO and f-rGO were fabricated and tested on cross flow filtration membrane cell. As illustrated in Fig. 9 pure water flux increases by the incorporation of rGO and f-rGO into the polymer matrices. The bare PES membrane, characterized by its finger-like structure, demonstrates a pure water flux of 148 ± 5.3 LMH ($L/m^2.h$ or LMH). This finger-like structure promotes water flow by establishing preferential routes for water molecules. The addition of rGO in to the PES membrane leads to increase in flux (Li and Tian, 2021), with a pure water flux value of 168 ± 3.0 LMH. The rise in pure water flux might be due to the increase in hydrophilicity and an enlargement of pore size (Hamzah *et al.* 2020), as evidenced by CA and SEM data. After the incorporation of f-rGO, the membrane's permeability was notably enhanced, reaching 257 ± 2.5 LMH for f-rGO/PES membrane. These increase in pure water flux was due to the addition of more hydrophilic f-rGO, which contain $-CH_2NH_2$ group leads to increase in hydrophilicity of the membrane. It is widely recognized that the increased hydrophilicity of the membranes can enhance water permeability by attracting water molecules into the membrane matrix and facilitating their passage through the membrane. These findings align with a prior investigation by Chai and colleagues, who suggested that the increase in flux values could be attributed to larger pore size, improved porosity, and enhanced hydrophilicity (Chai *et al.* 2017, Subtil *et al.* 2020).

3.8 Heavy metal removal study

Heavy metal rejection study of all the fabricated membranes were carried out at 50 psi transmembrane pressure in the membrane filtration cell by using 1000ppm solution of $Pb(NO_3)_2$, $CuSO_4$ and $K_2Cr_2O_7$ prepared in DM water. The percentage rejection of specific heavy metals is illustrated in Table 4. The percentage rejection of heavy metals for bare PES membrane was 13.0 ± 0.47% for Pb(II), 37.1 ± 0.33% for Cu(II) and 14.0 ± 0.85% for Cr(VI). The inclusion of rGO in the polymeric matrix further enhances its metal rejection properties. When rGO was added to PES membranes, the rejection rates experienced notable alterations. The integration of rGO into PES membranes, the rejection percentages shifted to 68.8 ± 0.32% for Pb(II), 80.3 ± 0.27% for Cu(II) and 85.6 ± 0.37% for Cr(VI). Further the incorporation of f-rGO into the polymer matrices, a notable enhancement in rejection percentage was observed. The incorporation of f-rGO led to the formation of amide linkage and additional functionalities, resulting in significant rejection rates: 88.5 ±0.19% for Pb(II), 92.0 ± 0.12% for Cu(II) and 95.3 ± 0.33% for Cr(VI).

According to the study, heavy metal ion rejection was greatly enhanced by adding rGO to PES membrane. This improvement was then further enhanced by adding f-rGO in place of rGO into the polymer matrix. rGO and amine-functionalized rGO membranes possess functional groups such as hydroxyl (-OH), carboxyl (-COOH), and amine (-NH2) groups on their surfaces. These functional groups enhance the affinity of the membrane for metal ions through complexation or chemical bonding, increasing the adsorption capacity and consequently improving rejection rates. The presence of amine functional groups facilitates electrostatic interactions with metal ions. This interaction can lead to stronger binding of metal ions to the membrane surface, further enhancing rejection rates of f-rGO/PES membrane (Mistry *et al.* 2023, Mistry and Murthy 2023, Shah and Murthy 2013).

3.9 Antifouling properties of the membranes

The percentage rejection of BSA was investigated by the filtration of 100 ppm BSA solution at 50 psi pressure. The antifouling properties of all the fabricated membranes were also investigated by calculating FRR and Rir. pristine PES membrane initially showed BSA rejection rate of 79.5 ± 1.2% along with FRR of 36.4 ± 2.5% and Rir of 63.6 ± 3.7%. Upon the incorporation of rGO into the polymer matrices, BSA rejection rates improved to 88.0 ± 0.5% for rGO/PES membrane, with FRR of 55.8 ± 1.8% and Rir value of 44.2 ±2.0%. Subsequently after the addition of f-rGO a notable enhancement was observed. f-rGO/PES membrane demonstrated outstanding BSA rejection, reaching 94.2 ± 0.7%, along with a FRR of 80.5 ± 1.3% and a Rir of 19.5 ± 1.6% (Fig. 10 (a)-(b)). The antifouling properties of membranes depend upon their higher hydrophilicity, surface roughness, altered surface charge, and prevention of pore blockage. Smoother and more hydrophilic membranes are needed to counteract the initial

Table 4 Pure water flux and heavy metal removal of pristine PES membrane and PES membranes embedded with rGO and f-rGO

Membranes	Pure water flux LMH	% rejection of metals		
		Pb (II)	Cu (II)	Cr (VI)
PES	148 ± 5.3	13.0 ± 0.47	37.1 ± 0.33	14.0 ± 0.85
rGO/PES	168 ± 1.2	68.8 ± 0.32	80.3 ± 0.27	85.6 ± 0.37
f-rGO/PES	257 ± 1.0	88.5 ± 0.19	92.0 ± 0.12	95.3 ± 0.33

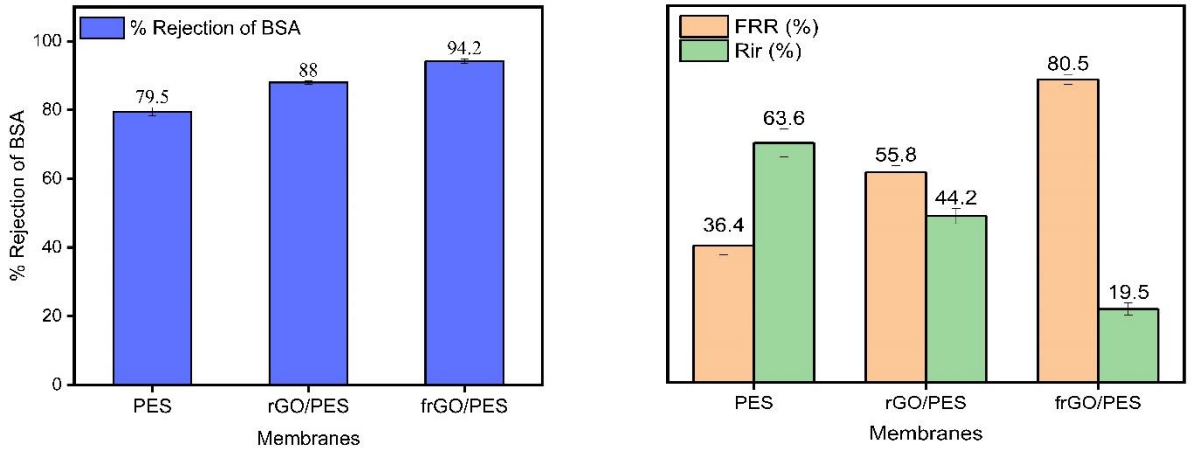

Fig. 10 Representation of fouling properties of all the fabricated membranes

fouling tendencies, because protein is hydrophobic. Hydrophilic membranes provide a water layer on their surfaces, which slows down the adsorption of organic foulants (Hwang *et al.* 2013, Vatanpour *et al.* 2012b). Additionally, it is well recognized that smoother membranes have greater antifouling capabilities since they have a lower probability for foulant attachment. Thus, the addition of rGO and f-rGO leads to an increase in hydrophilicity and decrease in surface roughness of the membrane, affects membrane performance dramatically.

4. Conclusions

This study presented the fabrication and characterization of mixed matrix membranes (MMMs) embedded with graphene derivatives (rGO and f-rGO) for enhanced filtration performance.

• The incorporation of rGO and f-rGO into polyethersulfone (PES) membranes resulted in significant improvements in pure water flux, heavy metal rejection, and protein fouling resistance.

• The introduction of amine functional groups during the synthesis of f-rGO further enhances membrane performance, leading to higher rejection rates and improved antifouling properties compared to rGO/PES membranes.

Overall, the study highlights the potential of graphene derivatives in enhancing the performance of membrane-based filtration systems, offering promising opportunities for applications in water treatment, wastewater remediation, and other separation processes.

Acknowledgments

The authors acknowledge the government of Gujarat for providing financial support (SHODH fellowship) during this study. Also, we acknowledge IIT Mumbai for SEM characterization, SAIF Kottayam for AFM characterization and Dr. Vickram Jeet Singh for his help with the CA measurement.

References

Abdalla, O., Wahab, M.A., and Abdala, A. (2020), "Mixed matrix membranes containing aspartic acid functionalized graphene oxide for enhanced oil-water emulsion separation", *J. Environ. Chem. Eng.*, **8**(5), 104269. https://doi.org/10.1016/j.jece.

Abdel-Karim, A., Luque-Alled, J.M., Leaper, S., Alberto, M., Fan, X., Vijayaraghavan, A., Gad-Allah, T.A., El-Kalliny, A.S., Szekely, G., Ahmed, S.I.A., Holmes, S.M. and Gorgojo, P. (2019), "PVDF membranes containing reduced graphene oxide: Effect of degree of reduction on membrane distillation performance", *Desalination*, **452**, 196-207. https://doi.org/10.1016/j.desal.2018.11.014.

Adetayo, A., Runsewe, D. (2019), "Synthesis and fabrication of graphene and graphene oxide: A review", *Open J. Compos. Mater.*, **9**(2), 207. https://doi.org/10.4236/ojcm.

Alam, J., Dass, L.A., Ghasemi, M. and Alhoshan, M. (2013), "Synthesis and optimization of PES-Fe3O4 mixed matrix nanocomposite membrane: Application studies in water purification", *Polym. Compos.*, **34**(11), 1870-1877. https://doi.org/10.1002/pc.22593.

Al-Naddaf, Q., Al-Mansour, M., Thakkar, H. and Rezaei, F. (2018), "MOF-GO hybrid nanocomposite adsorbents for

methane storage", *Ind. Eng. Chem. Res.*, **57**(51), 17470-17479. https://doi.org/10.1021/acs.iecr.8b03638.

Aziz, M., Tajul Arifin, N.F. and Lau, W.J. (2019), "Preparation and characterization of improved hydrophilic polyethersulfone/ reduced graphene oxide membrane", *Malaysian J. Anal. Sci.*, **23**(3), 479-487. https://doi.org/10.17576/mjas-2019-2303-12.

Bakshi, A., Bustamante, H., Sui, X. and Joshi, R. (2021), "Structure dependent water transport in membranes based on two-dimensional materials", *Ind. Eng. Chem. Res*., **60**(30), 10917-10959. https://doi.org/10.1021/acs.iecr.1c01919.

Barakat, M.A. (2011), "New trends in removing heavy metals from industrial wastewater", *Arab. J. Chem.*, **4**(4), 361-377. https://doi.org/10.1016/j.arabjc.2010.07.019.

Bhol, P., Yadav, S., Altaee, A., Saxena, M., Misra, P.K. and Samal, A.K. (2021), "Graphene-based membranes for water and wastewater treatment: a review", *ACS Appl. Nano Mater*., **4**(4), 3274-3293. https://doi.org/10.1021/acsanm.0c03439.

Bora, C., Bharali, P., Baglari, S., Dolui, S. and Konwar, B. (2013), "Strong and conductive reduced graphene oxide/polyester resin composite films with improved mechanical strength, thermal stability and its antibacterial activity", *Compos. Sci. Technol*., **87**, 1-7. https://doi.org/10.1016/j.compscitech.2013.07.025.

Celik, E., Park, H., Choi, H. and Choi, H. (2011), "Carbon nanotube blended polyethersulfone membranes for fouling control in water treatment", *Water Res.*, **45**(1), 274-282. https://doi.org/10.1016/j.watres.2010.07.060.

Chai, P.V., Mahmoudi, E., Teow, Y.H. and Mohammad, A.W. (2017), "Preparation of novel polysulfone-Fe3O4/GO mixed-matrix membrane for humic acid rejection", *J. Water Proc. Eng*., **15**, 83-88. https://doi.org/10.1016/j.jwpe.2016.06.001.

Das, E. and Yurtcan, A.B. (2022), "Synthesis of reduced graphene oxide (rGO) supported Pt nanoparticles via supercritical carbon dioxide deposition technique for PEM fuel cell electrodes", *J. Anatol. Phys. Astro.*, **2**(1), 1-17.

Forati, T., Atai, M., Rashidi, A.M., Imani, M. and Behnamghader, A. (2014), "Physical and mechanical properties of graphene oxide/polyethersulfone nanocomposites", *Polym. Adv. Technol*., **25**(3), 322-328. https://doi.org/10.1002/pat.3243.

Ganesh, B.M., Isloor, A.M. and Ismail, A.F. (2013), "Enhanced hydrophilicity and salt rejection study of graphene oxide-polysulfone mixed matrix membrane", *Desalination*, **313**, 199-207. https://doi.org/10.1016/j.desal.2012.11.037.

Giwa, A., Ahmed, M. and Hasan, S.W. (2019), *Polymeric Materials for Clean Water*, Springer, Cham, Switzerland.

Gohari, R.J., Halakoo, E., Lau, W.J., Kassim, M.A., Matsuura, T. and Ismail, A.F. (2014), "Novel polyethersulfone (PES)/ hydrous manganese dioxide (HMO) mixed matrix membranes with improved anti-fouling properties for oily wastewater treatment process", *RSC Adv*., **4**(34), 17587-17596. https://doi.org/10.1039/C4RA00032C.

Hamzah, N., Johary, F., Rohani, R., Sharifuddin, S.S. and Ise, M.H.M. (2020), "Development of polyethersulfone (PES) reduced graphene oxide nanocomposite nanofiltration membrane", *Malaysian J. Fund. Appl. Sci.*, **16**(4), 418-421. https://doi.org/10.11113/mjfas.v16n4.1613.

Hou, S., Su, S., Kasner, M.L., Shah, P., Patel, K. and Madarang, C.J. (2010), "Formation of highly stable dispersions of silane-functionalized reduced graphene oxide", *Chem. Phys. Lett.*, **501**(1-3), 68-74. https://doi.org/10.1016/j.cplett.2010.10.051.

Hwang, L.L., Chen, J.C. and Wey, M.Y. (2013), "The properties and filtration efficiency of activated carbon polymer composite membranes for the removal of humic acid", *Desalination*, **313**, 166-175. https://doi.org/10.1016/j.desal.2012.12.019.

Irani, V., Tavasoli, A. and Vahidi, M. (2018), "Preparation of amine functionalized reduced graphene oxide/methyl diethanolamine nanofluid and its application for improving the CO_2 and H_2S absorption", *J. Colloid Interf. Sci.*, **527**, 57-67. https://doi.org/10.1016/j.jcis.2018.05.018.

Jafari, A., Mortaheb, H.R. and Gallucci, F. (2022), "Performance of octadecylamine-functionalized graphene oxide nanosheets in polydimethylsiloxane mixed matrix membranes for removal of toluene from water by pervaporation", *J. Water Proc. Eng*., **45**, 102497. https://doi.org/10.1016/j.jwpe.2021.102497.

Jamil, N., Othman, N.H., Alias, N.H., Shahruddin, M.Z., Roslan, R.A., Lau, W.J. and Ismail, A.F. (2019), "Mixed matrix membranes incorporated with reduced graphene oxide (rGO) and zeolitic imidazole framework-8 (ZIF-8) nanofillers for gas separation", *J. Solid State Chem.*, **270**, 419-427. https://doi.org/10.1016/j.jssc.2018.11.028.

Jia, Z. and Wang, Y. (2015), "Covalently crosslinked graphene oxide membranes by esterification reactions for ions separation", *J. Mater. Chem. A*, **3**(8), 4405-4412. https://doi.org/10.1039/C4TA06193D.

Latorrata, S., Cristiani, C., Basso Peressut, A., Brambilla, L., Bellotto, M., Dotelli, G., Finocchio, E., Gallo Stampino, P. and Ramis, G. (2021), "Reduced graphene oxide membranes as potential self-assembling filter for wastewater treatment", *Minerals*, **11**(1), 15. https://doi.org/10.3390/min11010015.

Li, Y., Zhao, W., Weyland, M., Yuan, S., Xia, Y., Liu, H., Jian, M., Yang, J., Easton, C.D., Selomulya, C. and Zhang, X. (2019), "Thermally reduced nanoporous graphene oxide membrane for desalination", *Environ. Sci. Technol*., **53**(14), 8314-8323. https://doi.org/10.1021/acs.est.9b01914.

Li, Z. and Tian, Y. (2021), "Recent advances in graphene oxide membranes for water desalination", *E3S Web of Conf*., **308**, 01023. https://doi.org/10.1051/e3sconf/202130801023.

Lin, H., Liu, R., Dangwal, S., Kim, S.J., Mehra, N., Li, Y. and Zhu, J. (2018), "Permselective H_2/CO_2 separation and desalination of hybrid GO/rGO membranes with controlled pre-crosslinking", *ACS Appl. Mater. Interf.*, **10**(33), 28166- 28175. https://doi.org/10.1021/acsami.8b05296.

Liu, H., Wang, H. and Zhang, X. (2015), "Facile fabrication of freestanding ultrathin reduced graphene oxide membranes for water purification", *Adv. Mater*, **27**(2), 249-254. https://doi.org/10.1002/adma.201404054

Marcano, D.C., Kosynkin, D.V., Berlin, J.M., Sinitskii, A., Sun, Z., Slesarev, A., Alemany, L.B., Lu, W. and Tour, J.M. (2010), "Improved synthesis of graphene oxide", *ACS Nano*, **4**(8), 4806-4814. https://doi.org/10.1021/nn1006368.

Mistry, P. and Murthy, C.N. (2023), "Positively charged polysulfone and polyether sulfone mixed matrix membranes modified with polyethylenimine: enhancing heavy metal rejection and antifouling properties", *ACS EST Water*, **3**(12), 4168-4182. https://doi.org/10.1021/acsestwater.3c00585.

Mistry, P., Nikita, K., Aswal, V.K., Kumar, S. and Murthy, C.N. (2023) "Modification of surface characteristics of functionalized multi-walled carbon nanotubes containing mixed matrix membrane using click chemistry", *Desalin. Water Treat.*, **295**, 42-51. https://doi.org/10.5004/dwt.2023.29589.

Mondal, S., and Majumder, S.K. (2020), "Fabrication of the polysulfone-based composite ultrafiltration membranes for the adsorptive removal of heavy metal ions from their contaminated aqueous solutions", *Chem. Eng. J.*, **401**, 126036. https://doi.org/10.1016/j.cej.2020.126036.

Moradi, G., Zinadini, S. and Rajabi, L. (2020), "Development of the tetrathioterephthalate filler incorporated PES nanofiltration membrane with efficient heavy metal ions rejection and superior antifouling properties", *J. Environ. Chem. Eng.*, **8**(6), 104431. https://doi.org/10.1016/j.jece.2020.104431.

Mukherjee, R., Bhunia, P. and De, S. (2016), "Impact of graphene oxide on removal of heavy metals using mixed matrix membrane", *Chem. Eng. J.*, **292**, 284-297. https://doi.org/10.1016/j.cej.2016.02.015.

Mungse, H.P. and Khatri, O.P. (2014), "Chemically functionalized reduced graphene oxide as a novel material for reduction of friction and wear", *J. Phys. Chem. C*, **118**(26), 14394-14402.

https://doi.org/10.1021/jp5033614.
Nasrollahi, N., Aber, S., Vatanpour, V. and Mahmoodi, N.M. (2019), "Development of hydrophilic microporous PES ultrafiltration membrane containing CuO nanoparticles with improved antifouling and separation performance", *Mater. Chem. Phys.*, **222**, 338-350. https://doi.org/10.1016/j.matchemphys.2018.10.032.
Nikita, K., Ray, D., Aswal, V.K. and Murthy, C.N. (2020), "Surface modification of functionalized multiwalled carbon nanotubes containing mixed matrix membrane using click chemistry", *J. Membr. Sci.*, **596**, 117710. https://doi.org/10.1016/j.memsci.2019.117710.
Nompumelelo, K.S., Edward, N.N., Muthumuni, M., Moloko, M. and Makwena, M.J. (2023), "Fabrication, modification, and mechanism of nanofiltration membranes for the removal of heavy metal ions from wastewater", *Chemistry Select*, **8**(33), e202300741. https://doi.org/10.1002/slct.202300741.
Peyravi, M., Rahimpour, A., Jahanshahi, M., Javadi, A. and Shockravi, A. (2012), "Tailoring the surface properties of PES ultrafiltration membranes to reduce the fouling resistance using synthesized hydrophilic copolymer", *Micropor. Mesopor. Mater.*, **160**, 114-125. https://doi.org/10.1016/j.micromeso.2012.04.036.
Qasem, N., Mohammed, R. and Lawal, D. (2021), "Removal of heavy metal ions from wastewater: a comprehensive and critical review", *Npj Clean Water*, **4**(1), 1-15. https://doi.org/10.1038/s41545-021-00127-0.
Rahimpour, A. (2011), "UV photo-grafting of hydrophilic monomers onto the surface of nano-porous PES membranes for improving surface properties", *Desalination*, **265**(1-3), 93-101. https://doi.org/10.1016/j.desal.2010.07.037.
Rahimpour, A. and Madaeni, S.S. (2007), "Polyethersulfone (PES)/cellulose acetate phthalate (CAP) blend ultrafiltration membranes: Preparation, morphology, performance and antifouling properties", *J. Membr. Sci.*, **305**(1-2), 299-312. https://doi.org/10.1016/j.memsci.2007.08.030.
Razmjou, A., Resosudarmo, A., Holmes, R.L., Li, H., Mansouri, J. and Chen, V. (2012), "The effect of modified TiO_2 nanoparticles on the polyethersulfone ultrafiltration hollow fiber membranes", *Desalination*, **287**, 271-280. https://doi.org/10.1016/j.desal.2011.11.025.
Safarpour, M., Khataee, A. and Vatanpour, V. (2014), "Preparation of a novel polyvinylidene fluoride (PVDF) ultrafiltration membrane modified with reduced graphene oxide/titanium dioxide (TiO_2) nanocomposite with enhanced hydrophilicity and antifouling properties", *Ind. Eng. Chem. Res.*, **53**(34), 13370-13382. https://doi.org/10.1021/ie502407g.
Seman, M. A., Khayet, M. and Hilal, N. (2012), "Comparison of two different UV-grafted nanofiltration membranes prepared for reduction of humic acid fouling using acrylic acid and N-vinylpyrrolidone", *Desalination*, **287**, 19-29. https://doi.org/10.1016/j.desal.2010.10.031.
Shah, P. and Murthy, C.N. (2013), "Studies on the porosity control of MWCNT/polysulfone composite membrane and its effect on metal removal", *J. Membr. Sci.*, **437**, 90-98. https://doi.org/10.1016/j.memsci.2013.02.042.
Sharma, N., Sharma, V., Jain, Y., Kumari, M., Gupta, R., Sharma, S.K. and Sachdev, K. (2017), "Synthesis and characterization of graphene oxide (GO) and reduced graphene oxide (rGO) for gas sensing application", *Macromol. Symp.*, **376**(1), 1700006. https://doi.org/10.1002/masy.
Shen, L., Bian, X., Lu, X., Shi, L., Liu, Z., Chen, L., Hou, Z. and Fan, K. (2012), "Preparation and characterization of ZnO/ polyethersulfone (PES) hybrid membranes", *Desalination*, **293**, 21-29. https://doi.org/10.1016/j.desal.2012.02.019.
Sheshmani, S. and Fashapoyeh, M.A. (2013), "Suitable chemical methods for preparation of graphene oxide, graphene and surface functionalized graphene nanosheets", *Acta Chimica Slovenica*, **60**(4), 813-825.
Shi, Q., Su, Y., Chen, W., Peng, J., Nie, L., Zhang, L. and Jiang, Z. (2011), "Grafting short-chain amino acids onto membrane surfaces to resist protein fouling", *J. Membr. Sci.*, **366**(1-2), 398-404. https://doi.org/10.1016/j.memsci.2010.10.032.
Sogut, E.G., Karatas, Y., Gulcan, M. and Kilic, N.C. (2020), "Enhancement of adsorption capacity of reduced graphene oxide by sulfonic acid functionalization: Malachite green and Zn (II) uptake", *Materials Chemistry and Physics*, **256**, 123662. https://doi.org/10.1016/j.matchemphys.2020.123662.
Sonawane, S.H., Terrien, A., Figueiredo, A.S., Clara Goncalves, M. and De Pinho, M.N. (2017), "The role of silver nanoparticles on mixed matrix Ag/cellulose acetate asymmetric membranes", *Polym. Compos.*, **38**(1), 32-39. https://doi.org/10.1002/pc.23557.
Subtil, E.L., Goncalves, J., Lemos, H.G., Venancio, E.C., Mierzwa, J.C., de Souza, J.D.S., Alves, W. and Le-Clech, P. (2020), "Preparation and characterization of a new composite conductive polyethersulfone membrane using polyaniline (PANI) and reduced graphene oxide (rGO)", *Chem. Eng. J.*, **390**, 124612. https://doi.org/10.1016/j.cej.2020.124612.
Van der Bruggen, B. (2009), "Chemical modification of polyethersulfone nanofiltration membranes: A review", *J. Appl. Polym. Sci.*, **114**(1), 630-642. https://doi.org/10.1002/app.30578.
Vatanpour, V., Madaeni, S.S., Khataee, A.R., Salehi, E., Zinadini, S. and Monfared, H.A. (2012), "TiO_2 embedded mixed matrix PES nanocomposite membranes: Influence of different sizes and types of nanoparticles on antifouling and performance", *Desalination*, **292**, 19-29. https://doi.org/10.1016/j.desal.2012.02.006.
Vatanpour, V., Madaeni, S.S., Rajabi, L., Zinadini, S. and Derakhshan, A.A. (2012), "Boehmite nanoparticles as a new nanofiller for preparation of antifouling mixed matrix membranes", *J. Membr. Sci.*, **401**, 132-143. https://doi.org/10.1016/j.memsci.2012.01.040.
Vatanpour, V., Mousavi Khadem, S.S., Masteri-Farahani, M., Mosleh, N., Ganjali, M.R., Badiei, A., Pourbashir, E., Mashhadzadeh, A.H., Tajammal Munir, M., Mahmodi, G., Zarrintaj, P., Ramsey, J.D., Kim, S.J. and Saeb, M.R. (2020), "Anti-fouling and permeable polyvinyl chloride nanofiltration membranes embedded by hydrophilic graphene quantum dots for dye wastewater treatment", *J. Water Proc. Eng.*, **38**, 101652. https://doi.org/10.1016/j.jwpe.2020.101652.
Wu, G., Gan, S., Cui, L. and Xu, Y. (2008), "Preparation and characterization of PES/TiO_2 composite membranes", *Appl. Surf. Sci.*, **254**(21), 7080-7086. https://doi.org/10.1016/j.apsusc.2008.05.221.
Yang, E., Kim, C.M., Song, J.H., Ki, H., Ham, M.H. and Kim, I.S. (2017), "Enhanced desalination performance of forward osmosis membranes based on reduced graphene oxide laminates coated with hydrophilic polydopamine", *Carbon*, **117**, 293-300. https://doi.org/10.1016/j.carbon.2017.03.005.
Zhang, Q., Qian, X., Thebo, K.H., Cheng, H.M. and Ren, W. (2018), "Controlling reduction degree of graphene oxide membranes for improved water permeance", *Science Bulletin*, **63**(12), 788-794. https://doi.org/10.1016/j.scib.2018.05.015.
Zhou, X., Zhang, J., Wu, H., Yang, H., Zhang, J. and Guo, S. (2011), "Reducing graphene oxide via hydroxylamine: a simple and efficient route to graphene", *J. Phys. Chem. C*, **115**(24), 11957-11961. https://doi.org/10.1021/jp202575j.
Zinadini, S., Zinatizadeh, A.A., Rahimi, M., Vatanpour, V. and Zangeneh, H. (2014), "Preparation of a novel antifouling mixed matrix PES membrane by embedding graphene oxide nanoplates", *J. Membr. Sci.*, **453**, 292-301. https://doi.org/10.1016/j.memsci.2013.10.070.

CC